Proceedings of Combustion Institute - Canadian Section
Spring Technical Meeting
Queen's University
May 13-16, 2024

Computational Diagnostics of Diesel Spray End-of-Injection Combustion Recession

F.J. Arguelles*, M.D. Fagade, S.P. Hus, and X.H. Fang

Department of Mechanical and Manufacturing Engineering, University of Calgary, 40 Research Place NW, Calgary, AB, Canada, T2L 1Y6

Abstract

Diesel engines are efficient, reliable, and durable, making them a popular choice for ground transportation and heavy-duty applications. While emissions controls are challenging for diesel engines, strategies such as low-temperature combustion (LTC) strategies have been proven to reduce nitrogen oxides and particulate matter emissions that are common in diesel engines. However, these strategies can result in an increased fraction of the fuel spray being unburnt, leading to unburned hydrocarbon (UHC) emissions. Previous studies have indicated that end-of-injection (EOI) processes can support ignition near the nozzle, thereby consuming the UHCs after EOI. In particular, combustion recession is an EOI process where high-temperature ignition occurs between the nozzle and flame lift-off length, consuming UHCs in the process. Current literature suggests that combustion recession is likely attributed to auto-ignition rather than flame propagation. This is inferred through the analysis of the flame structures at different boundary conditions. However, previous studies have not presented a quantitative analysis of whether combustion recession is driven by auto-ignition or flame propagation. Chemical explosive mode analysis (CEMA) is a flame diagnostic tool based on the eigenanalysis for the chemical Jacobian to identify critical combustion events and has been used in various types of combustion setups, including LTC of diesel sprays. CEMA has been successfully used to determine flame features and is also able to identify the local propagation regimes within a flame which includes auto-ignition, deflagration, and extinction. Therefore, the objective of this study is to further the understanding of the combustion recession of diesel sprays through computational fluid dynamics (CFD) at LTC conditions where a customized CEMA is implemented to study the EOI combustion modes. The study involves large eddy simulations of a single-hole injection of n-dodecane in an Eulerian-Lagrangian framework performed in the CFD solver CONVERGE. The boundary conditions of the study are in the range of Engine Combustion Network's "Spray A" conditions. At the baseline boundary conditions of "Spray A", two chemical kinetic mechanisms are compared with experimental data. With the selected chemical mechanism, the custom implementation of CEMA is used to determine the flame features AEOI and the propagation regime of combustion recession to provide insight into the flame re-initiation mechanism. Through CEMA, it was determined that combustion recession is auto-ignition dominated: the reactive mixtures near the nozzle auto-ignite, and the ignited kernels develop through flame propagation. Lower ambient temperatures cannot support auto-ignition, which leads to the extinction of the flame near the nozzle.

1 Introduction

Diesel engines are efficient, reliable, and durable, making them a popular choice for ground transportation and heavy-duty applications. However, they emit large amounts of nitrogen oxides (NOx) and particulate matter (PM), both of which are detrimental to the environment. One of the strategies to reduce these emissions is low-temperature combustion (LTC), which involves reducing the overall temperature within the cylinder and increasing overall air-fuel mixing [1]. LTC strategies have been proven to reduce NOx and PM emissions [1], but they can also result in an increased fraction of the fuel spray being unburnt, leading to unburned hydrocarbons (UHCs). Thus, characterizing diesel sprays at LTC conditions may help understand the underlying processes involved in increased UHCs. End-of-injection (EOI) processes have been linked to emissions formation in diesel engines [2, 3]. Particularly, in a study by Knox et al. [4] to mitigate UHCs, they controlled the injection ramp-down rate and saw that second-stage high-temperature ignition (HTI) occurred near the injector nozzle, named

*Corresponding author: fransjoseph.arguelle@ucalgary.ca

combustion recession. Combustion recession is an EOI phenomenon where HTI occurs between the nozzle and flame lift-off length (FLOL), consuming UHCs in the process. Both experimental and numerical studies have shown that combustion recession can appear as separated pockets or a continuous stream of ignition propagating from the FLOL toward the fuel nozzle [4, 5]. Combustion recession was also found to be affected by ambient conditions such as temperature and oxygen concentration as well as injector conditions such as injection pressure and ramp-down rates [5, 6]. However, a common point in these studies is that combustion recession is likely attributed to auto-ignition rather than flame propagation [4, 6]. While this is inferred by the analysis of the flame structures at different combustion conditions, previous studies have not yet presented a quantitative analysis of whether combustion recession is driven by auto-ignition or flame propagation.

The objective of this study is to further the understanding of the combustion recession of diesel sprays through computational fluid dynamics studies at LTC conditions where a customized chemical explosive mode analysis (CEMA) is implemented in CONVERGE to study the EOI combustion modes. Large eddy simulation (LES) in an Eulerian-Lagrangian framework is used to simulate n-dodecane reacting spray in ECN "Spray A" boundary conditions [7] with a parametric variation of ambient temperature.

2 Methodology

LES in an Eulerian-Lagrangian framework was employed using the CFD solver CONVERGE 2.4. Adaptive mesh refinement of up to 4 embedding levels refined the cells based on subgrid velocity and temperature fluctuations to increase computational accuracy. Fixed grid embedding of 5 levels was also applied to a volume near the nozzle to increase the resolution and accuracy of the high-velocity liquid spray. The maximum cell count of the computational domain is 12 million. The base cell size for the computational domain was chosen as 1 mm with a minimum cell size of 31.25 μm. The injection parcels were modeled using the "blob" method. Droplet breakup and collision were modeled using the Kelvin-Helmholtz Rayleigh-Taylor (KH-RT) model and the No-Time-Counter (NTC) model, respectively. Combustion was modeled using the well-stirred reactor (WSR) model, SAGE [8]. WSR models assume that each cell is homogeneous and therefore calculate the mean reaction rates based on the Arrhenius equations. Consequently, SAGE ignores turbulent-chemistry interaction (TCI) and can potentially have large errors due to the nonlinearity of turbulent reacting flows. However, the error from omitting TCI can be substantially reduced by increasing grid resolution [9]. Utilizing SAGE in their reacting spray simulations, Pei et al. [10, 11] determined that a minimum grid size of 62.5 μm or smaller than the nozzle diameter yielded grid-convergent results that are comparable to experimental data. Given the chosen minimum grid size of 31.25 μm and results from Pei et al., SAGE can be capable of accurately modeling the reacting spray, and thus predict combustion recession.

Table 1 summarizes the parametric variations of the reacting spray simulations. The boundary conditions are based on ECN "Spray A" boundary conditions. The surrogate fuel, n-dodecane, is injected directly from a single nozzle with an outlet diameter of 90 μm to a cylindrical chamber with an ambient oxygen composition of 15% by volume. The fuel is injected with a temperature of 363 K and an injection pressure of 150 MPa. The total injected mass is 3.46 mg and the total injection duration is 1.54 ms. Two chemical kinetic mechanisms by Luo et al. [12] and Yao et al. [13] are employed. For the sake of brevity, they will be referred to as the Luo mechanism and Yao mechanism, respectively throughout the rest of the study.

To aid in analyzing the flame AEOI, an implementation of chemical explosive mode analysis (CEMA) in CONVERGE 2.4 is utilized for the reacting spray simulations. CEMA is a flame diagnostic tool based on the eigenanalysis for the chemical Jacobian, $\boldsymbol{J_\omega}$, to identify critical combustion events and has been used in various types of combustion setups, including LTC of diesel sprays [14, 15]. CEMA has been successfully used to determine flame features and is also able to identify the local propagation regimes within a flame which includes auto-ignition, deflagration, and extinction [16]. $\boldsymbol{J_\omega}$ is defined as:

$$\frac{\mathrm{D}\boldsymbol{\omega}(y)}{\mathrm{D}t} = \boldsymbol{J_\omega}\frac{\mathrm{D}y}{\mathrm{D}t} = \boldsymbol{J_\omega}(\boldsymbol{\omega}+\boldsymbol{s}),\ \boldsymbol{J_\omega} = \frac{\delta\boldsymbol{\omega}}{\delta y}, \tag{1}$$

where $\boldsymbol{\omega}$ is the chemical source term, $\boldsymbol{s}$ is the non-chemical source term, and y are scalar values such as species concentration and temperature. Chemical explosive modes are associated with a real positive eigenvalue, λ_e:

$$\lambda_\mathrm{e} = \boldsymbol{b}_\mathrm{e}\cdot\boldsymbol{J_\omega}\cdot\boldsymbol{a}_\mathrm{e}, \tag{2}$$

where $\boldsymbol{a}_e$ and $\boldsymbol{b}_e$ are the right and left eigenvectors, respectively. A chemical explosive mode is also considered to be non-reactive if $|\lambda_e| \leq 1$. $\boldsymbol{b}_e$ is used to find the chemical ($\phi_{\boldsymbol{\omega}}$) and diffusion ($\phi_{\boldsymbol{s}}$) source terms, where the ratio of these two is defined as a local combustion mode indicator (α):

$$\phi_{\boldsymbol{\omega}} \equiv \boldsymbol{b}_e \cdot \boldsymbol{\omega},\ \phi_{\boldsymbol{s}} \equiv \boldsymbol{b}_e \cdot \boldsymbol{s},\ \alpha = \frac{\phi_{\boldsymbol{s}}}{\phi_{\boldsymbol{\omega}}}. \tag{3}$$

Auto-ignition mode ($-1 \leq \alpha \leq 1$) is where chemistry dominates diffusion and promotes ignition; deflagration mode ($\alpha > 1$) is where diffusion dominates chemistry and promotes ignition; extinction mode ($\alpha < -1$) is where diffusion dominates chemistry and reverses the ignition process [16].

Ambient Temperature (K)	800, **900**, 1000
Ambient Pressure (MPa)	5.25, **6.09**, 6.62

Table 1: “Spray A” parametric variations of the test conditions [7]. Bold text denote baseline conditions.

3 Results and Discussions

3.1 Reacting Spray Validation

The numerical reacting spray results are validated first by comparing the ignition delay time (IDT) and FLOL to experimental results. As suggested by ECN [7], IDT and FLOL are measured through high-temperature chemiluminescence of the OH radical (OH*). Specifically, IDT and FLOL are the time and axial locations where 50% of the maximum OH* chemiluminescence intensity occurs, respectively. Similarly, numerical IDT and FLOL are defined by ECN as the time when maximum $\frac{\mathrm{dT}}{\mathrm{dt}}$ occurs and the axial distance where the OH mass fraction reaches 2% of the instantaneous maximum after flame stabilization, respectively [7]. Table 2 summarizes the numerical and experimental IDTs and FLOLs under “Spray A” baseline conditions. The IDTs of both chemical mechanisms are consistent with experimental data, with the Luo and Yao mechanisms having a slight overprediction and underprediction, respectively when compared to experimental data. The FLOL from the Yao mechanism is also consistent with experimental data; however, the Luo mechanism overpredicts the FLOL. The likely reasons for these observations are the Luo mechanism has lower chemical source term values [17–19] and the Yao mechanism has enhanced reactions that produce formyl radicals (HCO) [20]. HCO is a key species in producing hydroperoxyl radicals, which is a key species in tracking first-stage ignition [21]. Nonetheless, the numerical results are comparable to experimental data, which allows us to further analyze the reacting spray simulations with the two mechanisms.

	Luo	Yao	Experiment
IDT (ms)	0.487	0.377	0.400–0.440
FLOL (mm)	23.4	16.5	15.8–17.9

Table 2: Ignition delay times and flame lift-off lengths. Experimental data obtained from ECN [7].

3.2 Chemical Kinetic Mechanism Selection

To select the appropriate chemical mechanism for combustion recession and subsequent analysis through CEMA, numerical temperature contours after EOI (AEOI) at baseline conditions are compared to experimental schlieren imaging from Skeen et al. [22]. Figure 1a shows that both chemical mechanisms qualitatively match the experimental flame near the FLOL and predict combustion recession. Combustion recession with the Luo mechanism starts to appear as a small ignition kernel that gradually develops. Between 0.2 and 0.3 ms AEOI, the ignition kernel connects to the main flame which has been developing towards the nozzle. It is worth noting that the combustion recession is not the same as flashback, which occurs due to the flame speed exceeding the fuel-air velocity. More likely, the increased temperature and mixture fraction caused the mixture just before the main flame to auto-ignite. This is consistent with previous studies [5, 23] where combustion recession occurs near stoichiometric mixture fractions (denoted by the solid cyan line in Figure 1a) and higher temperatures.

Similarly, combustion recession with the Yao mechanism also occurs near stoichiometric mixture fractions and starts as a group of small ignition kernels which are seen at 0.2 ms AEOI. These kernels develop closer to the nozzle and separately from each other, which is in line with experimental findings [4, 22]. In addition, the simulation with the Yao mechanism qualitatively matches the schlieren imaging more closely than the simulation with the Luo mechanism. However, combustion recession in both simulations occurs earlier than in the experiment. Specifically for the Yao mechanism, this is likely due to the slightly earlier ignition delay due to its enhanced reactions as previously mentioned.

To further compare the two chemical mechanisms, Figure 1b shows hydroxyl (OH) and formaldehyde (CH_2O) mass fraction contours and OH* chemiluminescence imaging from Knox et al. [4]. OH and CH_2O are representative of high-temperature and low-temperature ignition, respectively. OH* is the radical version of OH and is just as robust in representing HTI [22]. 50% of the OH* chemiluminescence intensity is set as the saturation threshold (shown in red) [4]. Similar observations from the temperature contours can be inferred from the evolution of species mass fractions. CH_2O concentrations propagate to leaner regions and are consumed in the process. From the consumption of CH_2O, HTI kernels then develop between the nozzle AEOI, indicated by red arrows in the figure. Interestingly, OH is concentrated around the periphery of these kernels. This is likely due to combustion reactions occurring at the flame front, which in the case of combustion recession, is the periphery of the kernel. Another likely reason is that the omission of TCI in WSR models produces higher OH concentrations in stoichiometric conditions, resulting in thin reaction zones [24]. The simulation with the Yao mechanism matches OH concentrations more closely with OH* chemiluminescence imaging and predicts reacting spray characteristics such as IDT and FLOL better. It also predicts combustion recession in baseline conditions as separated kernels as seen in previous studies. For these reasons, the Yao mechanism will be exclusively used for further analysis of the combustion modes determined through CEMA.

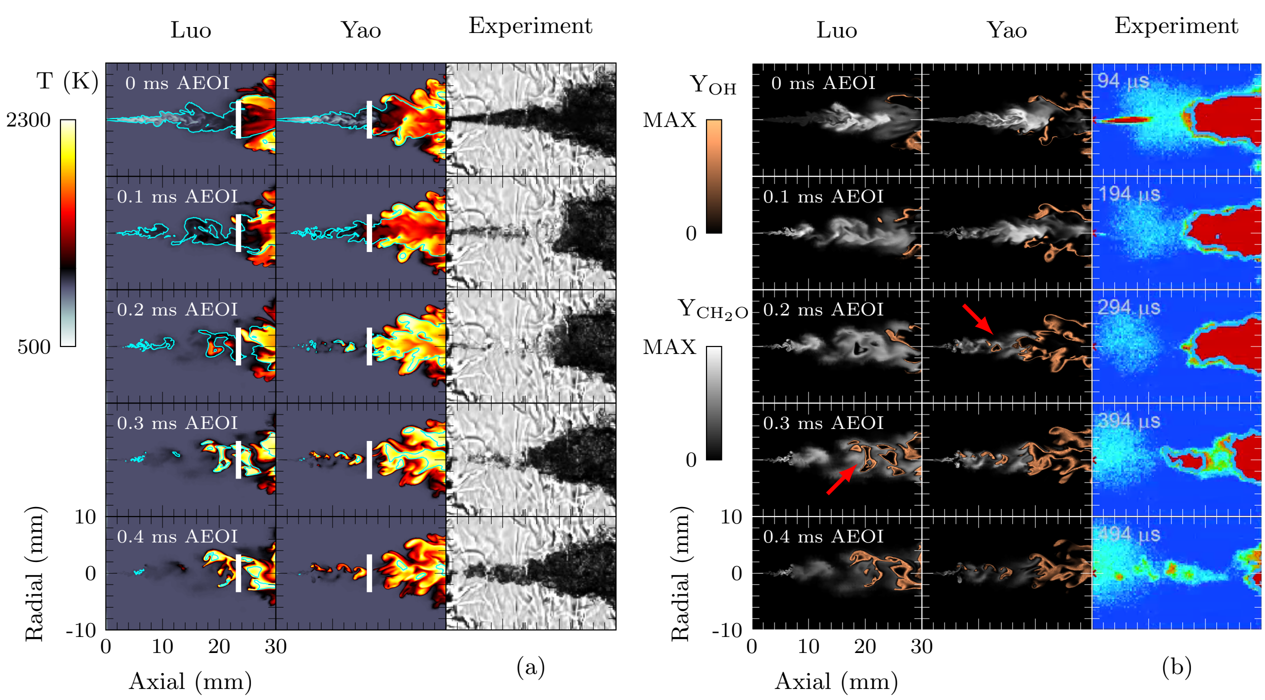

Fig. 1: Temperature contours and species mass fractions using two different chemical kinetic mechanisms compared with experimental schlieren imaging by Skeen et al. [22] (a) and experimental OH* chemiluminescence imaging by Knox et al. [4] (b). The solid vertical white line denotes FLOL AEOI. The timestamps in the chemiluminescence imaging is after start of ramp-down (ASORD). EOI is approximately 0.1 ms ASORD.

3.3 Chemical Explosive Mode Analysis with Ambient Temperature Variation

CEMA is utilized to determine the local combustion modes of the reacting spray AEOI, shown in Figure 2. In all ambient temperature variation cases, auto-ignition modes are dominant just AEOI. In the baseline case, auto-ignition modes coincide with the ignition kernels forming towards the nozzle, supporting previous findings that combustion recession is auto-ignition dominated. Interestingly, the ignition kernels start to increase in size where the deflagration modes are located. Conversely, combustion recession in the 1000 K case occurs and grows much more rapidly. It also appears as a continuous stream propagating back towards the nozzle. These observations are in line with previous experimental findings by Knox et al. [4]. In contrast to the baseline case, the deflagration modes are much more prominent in the 1000 K case. However, this is likely due to the increased reaction rate of HTI, thus "depleting" auto-ignition modes relatively fast.

A study by Gong et al. [25] found that auto-ignition induced flame fronts (AIIFs) are HTI sites that are prominently seen in inner fuel-rich zones. They also found two flame stabilization mechanisms where their relative importance is dependent on ambient temperatures [25]. At low ambient temperatures, the flame stabilizes due to auto-ignition with an AIIF at the flame base [25]. At high ambient temperatures, flame propagation is coupled with low-temperature ignition [25]. These observations are seen in the combustion events AEOI. In both the 900 K and 1000 K cases, the reactive mixtures between the nozzle and FLOL auto-ignite. Subsequently, the ignited kernels grow and develop through flame propagation, consuming CH_2O in the process, where the reaction rate is faster at higher ambient temperatures.

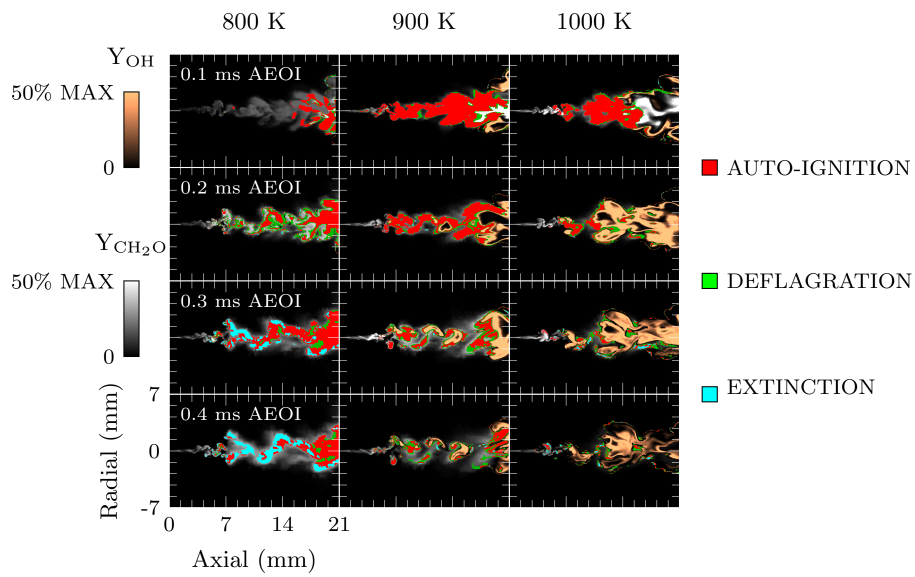

Fig. 2: Combustion modes near the nozzle AEOI determined by CEMA overlaid on species mass fractions.

The 800 K case does not show any signs of combustion recession, in line with previous experiments [4, 6]. As previously mentioned, auto-ignition modes occur just AEOI in the 800 K case. However, they do not occur near the nozzle (aside from a small auto-ignition mode kernel at 0.1 ms AEOI). Suddenly, at 0.2 ms AEOI, deflagration-dominated combustion modes start to appear near the nozzle. Between 0.2 and 0.3 ms AEOI, the deflagration modes start to convert into extinction modes. By 0.4 ms AEOI, the extinction modes dominate the area between the nozzle and the main flame. A likely reason for these observations is that the lower ambient temperatures cannot support auto-ignition, the main driving force of combustion recession. Without the initial onset of auto-ignition, the reactants over-mix and prevent ignition [2], explaining the transition from deflagration modes to extinction modes.

4 Conclusion

In this study, LES of an n-dodecane spray flame at "Spray A" boundary conditions are used to study the combustion recession phenomenon AEOI. Two chemical kinetic mechanisms are used with the WSR model, SAGE, in CONVERGE 2.4 to simulate the reacting spray. The Yao mechanism better predicts IDT and FLOL at baseline conditions. It also depicts combustion recession more closely to experimental observations. The simulations with the Yao mechanism are then analyzed through CEMA and a parametric variation of temperature. CEMA is found to be useful in determining the local combustion modes of an n-dodecane spray flame at LTC conditions AEOI. Through CEMA, it is determined that the combustion recession is auto-ignition dominated: the reactive mixtures found near the nozzle auto-ignite. After auto-ignition, the ignited kernels then develop due to flame propagation. Additionally, flame propagation is much more prevalent in higher ambient temperatures, whereas the mixtures in lower ambient temperatures cannot auto-ignite due to low reactivity. This leads to over-mixing and subsequent extinction of the flame. Future work includes further parametric variations and analysis of the extinction modes at lower ambient temperatures, which also includes a scalar dissipation rate study. Combustion models with TCI will also be implemented to study the effect of TCI on such AEOI phenomenon.

Acknowledgments

We gratefully acknowledge the financial support provided by the Natural Sciences and Engineering Research Council of Canada and Alberta Innovates. This research was enabled in part by support provided by the Research Computing Services group at the University of Calgary.

References

[1] T. Pachiannan, W. Zhong, S. Rajkumar, Z. He, X. Leng, Q. Wang, A literature review of fuel effects on performance and emission characteristics of low-temperature combustion strategies, Applied Energy 251 (2019) 113380.

[2] M. P. Musculus, T. Lachaux, L. M. Pickett, C. A. Idicheria, End-of-injection over-mixing and unburned hydrocarbon emissions in low-temperature-combustion diesel engines, Tech. rep., SAE Technical Paper (2007).

[3] N. Maes, M. Meijer, N. Dam, B. Somers, H. B. Toda, G. Bruneaux, S. A. Skeen, L. M. Pickett, J. Manin, Characterization of spray a flame structure for parametric variations in ecn constant-volume vessels using chemiluminescence and laser-induced fluorescence, Combustion and Flame 174 (2016) 138–151.

[4] B. W. Knox, C. L. Genzale, L. M. Pickett, J. M. Garcia-Oliver, W. Vera-Tudela, Combustion recession after end of injection in diesel sprays, SAE International Journal of Engines 8 (2) (2015) 679–695.

[5] M. Zhang, J. C. Ong, K. M. Pang, S. Xu, Y. Zhang, A. Nemati, X.-S. Bai, J. H. Walther, Large eddy simulation of combustion recession: Effects of ambient temperature and injection pressure, Fuel 351 (2023) 128831.

[6] B. W. Knox, C. L. Genzale, Scaling combustion recession after end of injection in diesel sprays, Combustion and Flame 177 (2017) 24–36.

[7] Sandia National Laboratories, Engine combustion network, `https://ecn.sandia.gov/`.

[8] P. Senecal, E. Pomraning, K. Richards, T. Briggs, C. Choi, R. McDavid, M. Patterson, Multi-dimensional modeling of direct-injection diesel spray liquid length and flame lift-off length using cfd and parallel detailed chemistry, SAE transactions (2003) 1331–1351.

[9] Convergent Science, Resolving turbulence-chemistry interactions in mixing-controlled combustion with les and detailed chemistry, White Paper (2023).

[10] Y. Pei, S. Som, E. Pomraning, P. K. Senecal, S. A. Skeen, J. Manin, L. M. Pickett, Large eddy simulation of a reacting spray flame with multiple realizations under compression ignition engine conditions, Combustion and Flame 162 (12) (2015) 4442–4455.

[11] Y. Pei, B. Hu, S. Som, Large-eddy simulation of an n-dodecane spray flame under different ambient oxygen conditions, Journal of Energy Resources Technology 138 (3) (2016) 032205.

[12] Z. Luo, S. Som, S. M. Sarathy, M. Plomer, W. J. Pitz, D. E. Longman, T. Lu, Development and validation of an n-dodecane skeletal mechanism for spray combustion applications, Combustion theory and modelling 18 (2) (2014) 187–203.

[13] T. Yao, Y. Pei, B.-J. Zhong, S. Som, T. Lu, K. H. Luo, A compact skeletal mechanism for n-dodecane with optimized semi-global low-temperature chemistry for diesel engine simulations, Fuel 191 (2017) 339–349.

[14] S. Zhong, S. Xu, F. Zhang, Z. Peng, L. Chen, X.-S. Bai, Cool flame wave propagation in high-pressure spray flames, Proceedings of the Combustion Institute 39 (2) (2023) 2513–2522.

[15] M. Gadalla, S. Karimkashi, I. Kabil, O. Kaario, T. Lu, V. Vuorinen, Embedded direct numerical simulation of ignition kernel evolution and flame initiation in dual-fuel spray assisted combustion, Combustion and Flame 259 (2024) 113172.

[16] C. Xu, J.-W. Park, C. S. Yoo, J. H. Chen, T. Lu, Identification of premixed flame propagation modes using chemical explosive mode analysis, Proceedings of the combustion Institute 37 (2) (2019) 2407–2415.

[17] X. Fang, R. Ismail, M. Davy, A study on kinetic mechanisms of diesel fuel surrogate n-dodecane for the simulation of combustion recession, Tech. rep., SAE Technical Paper (2019).

[18] X. Fang, R. Ismail, N. Sekularac, M. Davy, On the prediction of Spray A end of injection phenomenon using conditional source-term estimation, in: WCX SAE World Congress Experience, SAE International, 2020.

[19] X. Fang, N. Sekularac, M. H. Davy, Parametric studies of a novel combustion modelling approach for low temperature diesel spray simulation ASME 2020 Internal Combustion Engine Division Fall Technical Conference (2020) V001T06A005.

[20] J. M. Desantes, V. Bermúdez, J. J. López, D. López-Pintor, A new method to predict high and low-temperature ignition delays under transient thermodynamic conditions and its experimental validation using a rapid compression-expansion machine, Energy conversion and management 123 (2016) 512–522.

[21] J. M. Desantes, J. J. López, J. M. García-Oliver, D. López-Pintor, Experimental validation and analysis of seven different chemical kinetic mechanisms for n-dodecane using a rapid compression-expansion machine, Combustion and Flame 182 (2017) 76–89.

[22] S. A. Skeen, J. Manin, L. M. Pickett, Simultaneous formaldehyde plif and high-speed schlieren imaging for ignition visualization in high-pressure spray flames, Proceedings of the Combustion Institute 35 (3) (2015) 3167–3174.

[23] X. H. Fang, R. Ismail, K. Bushe, M. Davy, Simulation of ecn diesel spray a using conditional source-term estimation, Combustion Theory and Modelling 24 (4) (2020) 725–760.

[24] S. Kim, D. Jarrahbashi, C. Genzale, The role of turbulent-chemistry interaction in simulating end-of-injection combustion transients in diesel sprays, Tech. rep., SAE Technical Paper (2017).

[25] C. Gong, M. Jangi, X.-S. Bai, Large eddy simulation of n-dodecane spray combustion in a high pressure combustion vessel, Applied energy 136 (2014) 373–381.